Single Chloride Channels from *Torpedo* Electroplax

Activation by Protons

WOLFGANG HANKE and CHRISTOPHER MILLER

From the Department of Biochemistry, Brandeis University, Waltham, Massachusetts 02254

ABSTRACT Single-channel fluctuations of a chloride-specific channel from *Torpedo californica* electroplax were studied with high current and time resolution. Channels were incorporated into virtually solvent-free planar bilayer membranes formed from phospholipid monolayers, and the substructure of the open channel was analyzed. The single channel displays three well-defined substates of conductances 0, 10, and 20 pS in 200 mM Cl^-. These three substates are interpreted in terms of a dimeric channel complex composed of two identical "protochannels" gating independently in parallel on a time scale of milliseconds, but coupled together by a bursting process on a time scale of seconds. The probability of forming an open protochannel is voltage dependent and is increased strongly as aqueous pH is lowered. Variations of pH are effective only on the same side of the bilayer as the addition of electroplax vesicles. The dependence of single-channel kinetics on pH and voltage lead to a minimal four-state model in which both open and closed states can be protonated on a residue that changes its pK from 6 to 9 upon opening of the protochannel.

INTRODUCTION

The electroplax organ of the marine electric ray *Torpedo californica* carries an ion channel highly specific for Cl ion (Miller and White, 1980). Purification studies indicate that this channel resides in the noninnervated-face plasma membrane of the electroplax cell (White, 1981). The channel has been studied by insertion of noninnervated-face membrane vesicles into planar bilayer membranes (White and Miller, 1979, 1981*a*; Miller and White, 1980; Miller, 1982), by anion flux measurements on these vesicles (Taguchi and Kasai, 1980; White and Miller, 1981*b*), and by patch-recording from liposomes containing detergent extracts of the

Address reprint requests to Dr. Christopher Miller, Graduate Dept. of Biochemistry, Brandeis University, Waltham, MA 02254. Dr. Hanke's present address is Lehrstuhl für Zellphysiologie ND4, Ruhr-Universität Bochum, D-463 Bochum, Federal Republic of Germany.

J. GEN. PHYSIOL. © The Rockefeller University Press · 0022-1295/83/07/0025/21 $1.00 25
Volume 82 July 1983 25–45

noninnervated-face membranes (Tank et al., 1982; Tank and Miller, 1983). The channel displays two types of voltage-dependent gating processes: a slow process, on a time scale of seconds, and a fast process occurring in milliseconds. When single Cl^- channels are examined at high time resolution (Miller, 1982), it can be seen that channels appear in "bursts," that burst formation occurs on the second time scale, and that within a burst, rapid gating occurs among three well-defined conductance states. Burst formation has been thus identified with the slow gating process studied previously (White and Miller, 1979; Miller and White, 1980), whereas the multi-state fluctuations within a burst are responsible for the rapid process.

This study is concerned with the rapid gating process. It has previously been shown (Miller, 1982) that the three "substates" of the channel seen within a burst can be understood in terms of a dimeric model of the channel protein complex. The protein is viewed as a dimer of two identical "protochannels," each of which gates on the millisecond time scale between two states, open and closed. Three distinct conductance states are thus generated, corresponding to the opening of zero, one, or two of these protochannels. Assuming that the three substates are in fact attributable to the dimeric mechanism, it is possible to derive the probability of opening of the individual protochannel, as well as its rate constants of opening and closing (Miller, 1982). We have found that these fundamental protochannel parameters are profoundly affected by the pH of the aqueous phase; it is our intention here to characterize this effect quantitatively. We show that protons activate the rapid opening of the Cl^- channel, and we offer a minimal four-state model to account for both the voltage dependence and the activation by protons.

MATERIALS AND METHODS

Plasma membrane vesicles from *T. californica* electroplax were prepared from fresh tissue immediately after dissection, by fractionation on sucrose density gradients (Sobel et al., 1977). The light fraction, which is enriched in vesicles derived from the noninnervated face of the electroplax cell (White, 1981), was collected. The preparation was stored at −70°C in 0.4 M sucrose in small aliquots, each of which was thawed only once, on the day of the experiment.

Lipids used to form bilayers were phosphatidylethanolamine (PE) and phosphatidylcholine (PC) prepared from egg yolks (Labarca et al., 1980).

Planar Bilayers and Channel Insertion

Planar bilayers were formed according to Montal and Mueller (1972), using 6-μm-thick teflon partitions with holes of ~150 μm diam. Partitions were pretreated with *n*-hexadecane (5% in *n*-pentane) and allowed to dry in air. In all experiments, lipid monolayers were formed at the aqueous-air interface from a solution of 8 mM PE/2 mM PC in *n*-pentane; pentane was allowed to evaporate from the monolayers for at least 5 min before bilayer formation. The aqueous phases were 200 mM NaCl/10 mM Hepes, adjusted to the experimental pH with either NaOH or Tris base.

Chloride channels were inserted into the bilayer by adding vesicles (1–5 μg/

ml) to the *cis* aqueous solution, with continuous stirring, in the presence of 500 mM urea, also added to the *cis* chamber. In contrast to channel insertion into decane-containing bilayers (Miller and White, 1980), the transmembrane osmotic gradient established by urea addition was required here, with solvent-free bilayers. This requirement has also been observed in the fusion of liposomes with planar bilayers (Cohen et al., 1980, 1982). Channel insertion was monitored by measurement of conductance at a holding potential of −30 mV. After the first "fusion" event (detected as an abrupt increase in bilayer conductance), the *cis* chamber was extensively perfused with urea-free solution to re-establish symmetrical aqueous conditions and to inhibit further vesicle fusion. Only membranes containing a single Cl^- channel were used for data analysis; if more than one Cl^- channel was inserted in the first fusion event, the membrane was broken and a new attempt was made. To obtain a high probability of obtaining single-channel membranes, it was necessary to sonicate the vesicles for 2 min before use (Miller, 1982). All experiments were conducted at room temperature, 20–22°C.

The basic electrical setup has been described (Miller, 1982). Voltage was applied to the *cis* aqueous solution (the opposite, *trans* side was defined as ground) with an adjustable battery or function generator. The current across the bilayer was recorded using a fast current-to-voltage transducer (10 GΩ feedback resistance) based on a OPA101 amplifier (Burr-Brown Research Corp., Tucson, AZ). Feedback capacitance was compensated, and a high-frequency booster circuit was used (Hamill et al., 1981). The current was stored on FM tape for subsequent analysis.

Data Analysis

Data from FM tape were filtered at 0.5–1 kHz and sampled at 0.5–1 kHz by a MINC 11/23 computer (Digital Equipment Co., Maynard, MA). A pattern recognition program was then applied to the digitized records to identify the segments of time spent in the three open-channel substates. The collection of the following time segments was used to calculate for each of the three substates: time distribution, mean dwell time, long-term frequency of appearance, and mean conductance. Each time distribution was fit with a single-exponential relaxation, the time constant of which was compared with the mean dwell time of the same data set. There were two serious limitations on the data analysis. First, since the channel is rather small (10 pS), voltages smaller than 40 mV were usually not usable for the signal-to-noise ratio required for reliable automatic analysis. This made it impossible to analyze data between pH 9 and 10. Second, at highly negative voltages and low pH values, the rate of the "slow" gating process became fast enough to contaminate the fast process significantly; in this case, it was necessary to analyze the dwell-time distributions with double-exponential relaxations, using the faster component as a measure of the true substate fluctuations. In these cases, the amplitude of the slow fraction was never more than 10% of the total relaxation amplitude. Data were collected for analysis only from long-lasting bursts, i.e., bursts in which at least 100 substate fluctuations occurred.

RESULTS

Single chloride channels from *Torpedo* electroplax, when examined at 1 ms time resolution, display a characteristic "bursting" pattern, in which

long silent periods alternate with "active" periods (Fig. 1). During an active period, the channel fluctuates rapidly among three substates, named U, M, and D, with conductances 20, 10, and 0 pS in 200 mM Cl^-, respectively. The fact that these three substates always appear and disappear together identifies this three-level burst as the conducting unit of the Cl^- channel protein and appears to indicate rather complicated multistate behavior of the channel. However, a simple explanation of the three substates has been presented (Miller, 1982): a dimeric model in which the channel complex is composed of two identical, physically distinct Cl^-

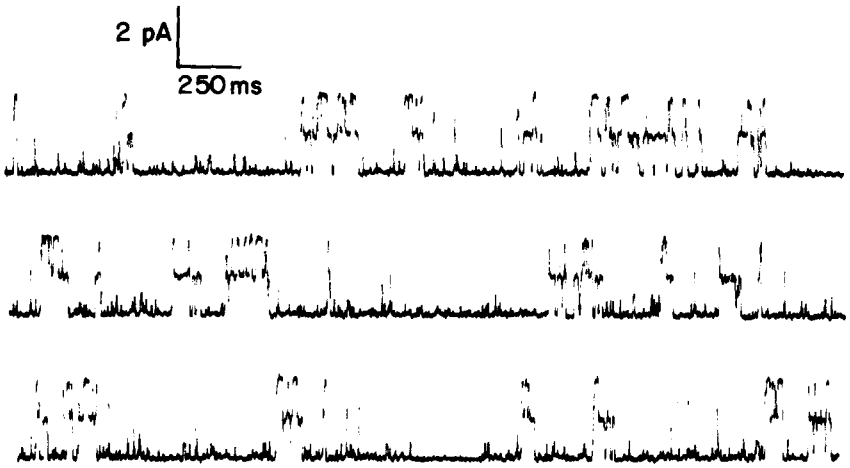

FIGURE 1. Dimeric bursts of Cl^- channels. A single Cl^- channel was inserted into a Montal-Mueller bilayer as described in Materials and Methods, and current was measured at −120 mV holding potential. In all traces in this report, upward deflection corresponds to channel opening.

diffusion pathways, or "protochannels." Each of the protochannels undergoes transitions between an open and a closed state; the three equally spaced substates represent the opening of both, one, or neither of the two protochannels. The fluctuating protochannels appear and disappear together via a second gating process operating on a slower time scale.

Our purpose here is threefold. First, we wish to subject the above dimeric picture of the rapid gating process to more extensive quantitative tests than previously presented. Second, we document the strong effect of the pH of the aqueous medium on the rapid gating behavior. Finally, we infer from the substate fluctuations of the channel complex a kinetic model for the individual protochannel's gating process.

Tests of Dimeric Gating Model

If we do not consider the long closed intervals between channel bursts, transitions among the channel's three substates can be formalized in terms of the dimeric model via scheme 1:

$$U \underset{\lambda}{\overset{2\mu}{\rightleftharpoons}} M \underset{2\lambda}{\overset{\mu}{\rightleftharpoons}} D. \quad (1)$$

Here, the rate constants λ and μ represent the fundamental opening and closing rates of each individual protochannel. This scheme makes several strong predictions concerning the probabilities of appearance of the substates and the rates of transition among them. We define the frequency of the ith substate, f_i, as the probability of observing that state within a burst. It is directly measurable from the fraction of time the channel spends in the ith substate. Then, if the protochannels are identical and independent in their rapid gating, it is required that the substate frequencies be binomially distributed:

$$f_D = (1 - p)^2 \qquad f_M = 2p(1 - p) \qquad f_U = p^2, \quad (2)$$

where p is the fundamental probability of an individual protochannel being in its open state, the "activation probability"; it is also directly measurable:

$$p = (f_M + 2f_U)/2. \quad (3)$$

Furthermore, the mean dwell times, $\bar{\tau}_i$, in the three sublevels can be written by inspection of scheme 1:

$$\bar{\tau}_D = \tfrac{1}{2}\lambda \qquad \bar{\tau}_M = 1/(\lambda + \mu) \qquad \bar{\tau}_U = \tfrac{1}{2}\mu. \quad (4)$$

Finally, the activation probability is related to the rate constants:

$$p/(1 - p) = \lambda/\mu; \quad (5)$$

this quantity is the observed equilibrium constant for opening. Therefore, from Eqs. 4 and 5, the two rate constants λ and μ are overdetermined from the four measurable quantities τ_D, τ_M, τ_U, and p:

$$\lambda = \tfrac{1}{2}\bar{\tau}_D \qquad \mu = \tfrac{1}{2}\bar{\tau}_U; \quad (6)$$

$$\lambda = p/\bar{\tau}_M \qquad \mu = (1 - p)/\bar{\tau}_M. \quad (7)$$

The scheme thus demands that the rate constants calculated from these independent measurements agree.

Table I shows a sample computer analysis of substate fluctuations within a burst, at a single voltage and pH. The measured frequencies, f_i, follow the *a priori* prediction of a binomial distribution, Eq. 2, within 5%. The rate constants agree within 10% whether calculated from Eq. 6 or Eq. 7. Finally, the three substates are equally spaced in conductance, within 5%. It is also important to realize that the mean dwell times agree well with the time constant of the exponential distribution of dwell times. The data of Table I are presented as an example representative of our experience with the system, over the entire range of pH and voltage used here. We conclude from these tests that the dimeric model is sufficient to explain the three-state fluctuations of the channel, and that we can use the observed transitions among these substates to extract the fundamental gating parameters of the single protochannel.

Dependence of Gating Probability on Voltage and pH

The Cl^- channel substate fluctuations show a pronounced voltage dependence (Fig. 2). At a fixed pH, as voltage is made more negative, the lower conductance substates are increasingly favored at the expense of the higher. In terms of the dimeric model, the protochannel activation probability increases with voltage, and this probability follows the prediction of a two-state channel model (Ehrenstein et al., 1970; Labarca et al.,

TABLE I

Analysis of Single-Channel Substate Fluctuations

Measured values	Substate		
	D	M	U
$\bar{\tau}$ (ms)	14.6 (14.1)	9.8 (8.5)	8.3 (7.9)
f	0.40 (0.39)	0.44 (0.47)	0.16 (0.14)
γ (pS)	0	10.4±0.3	21.1.±0.4

Calculated values	Equation used
$p = 0.38$	3
$\lambda = 36\ s^{-1}$	6
$\lambda = 40\ s^{-1}$	7
$\mu = 63\ s^{-1}$	6
$\mu = 67\ s^{-1}$	7

This table presents an analysis of a single data set typical of the data to be used here. A single channel was examined at −100 mV, pH 7.5. Protochannel activation probability p was measured from the substate frequencies f using Eq. 3. This value was then used to calculate the substrate frequencies predicted by a binomial distribution (shown in parentheses). Mean dwell times in the three substates, $\bar{\tau}$, were calculated directly and are compared with least-squares regression-line time constants of the dwell time distributions (in parentheses). Rate constants of opening, λ, and closing, μ, were calculated via Eq. 6 or Eq. 7, as indicated. Substate conductances, γ, are also shown.

1980), in which an equivalent charge, z, moves across the membrane upon channel opening (Fig. 4):

$$p(V) = [1 + e^{-zF(V-V_o)/RT}]^{-1}. \quad (8)$$

For the data of Fig. 2 (recorded at pH 7.0), $z = 1.1$ and the half-saturation voltage, V_o, is −85 mV. The protochannel therefore appears to gate by a simple mechanism involving only two conformational states, open and closed.

The aqueous pH also controls the channel's substate gating (Fig. 3). In these records, the pH was varied, while voltage was held fixed. It is apparent that lowering the pH tends to drive the protochannel open, whereas raising it has the opposite effect. The channel conductance is independent of pH in this range. In Fig. 4, the effects of both voltage and pH on the fundamental opening probability are shown. At each pH value, the probability-voltage curve follows Eq. 8. Lowering the pH

progressively shifts V_o toward more negative values, but z changes only slightly, from 1.3 at high pH to ~1.0 at low pH (Fig. 5). This pH-driven shift in V_o, ~60 mV per pH unit, is the basis for the "proton activation" of the chloride channel. By examining the pH dependence of the apparent equilibrium constant for opening via Hill plots (e.g., Fig. 6), we obtain an

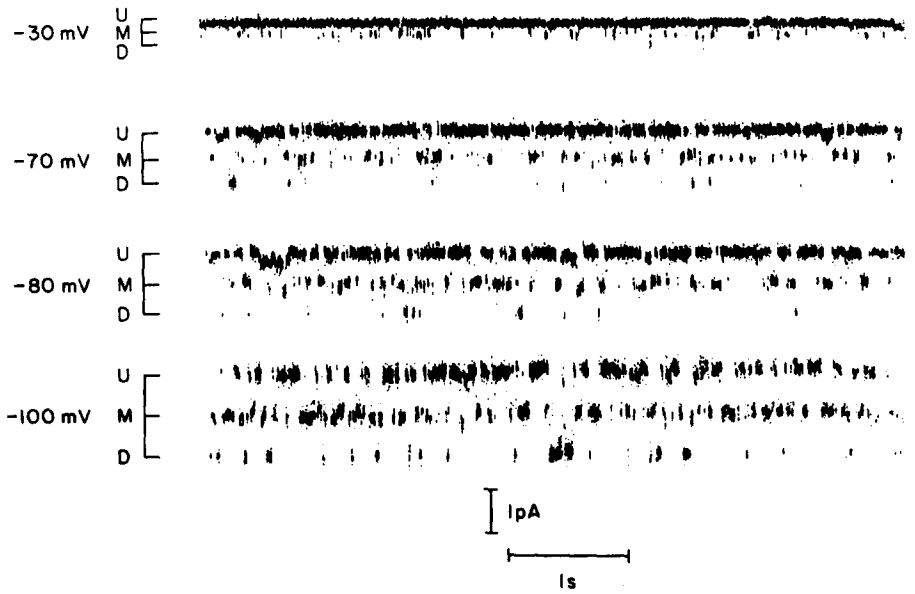

FIGURE 2. Voltage dependence of Cl^- channel substates. Substate fluctuations of a single Cl^- channel are shown at the indicated voltages, with a solution pH of 7.0. The currents corresponding to the three substates D, M, and U are marked. These traces were all taken from the same bilayer.

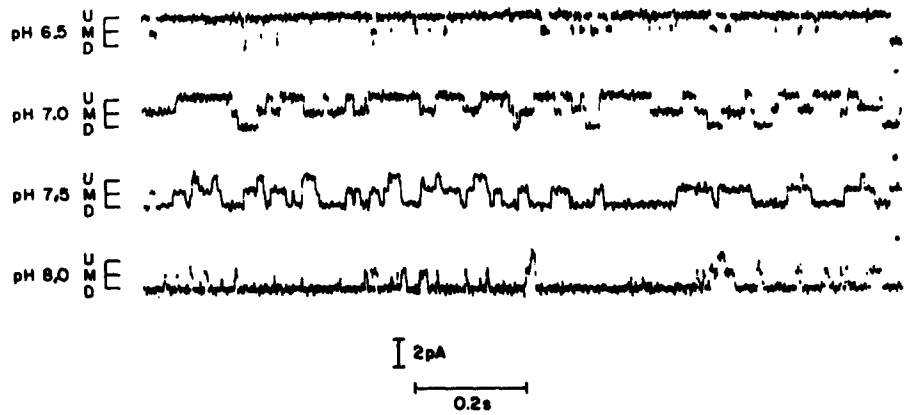

FIGURE 3. Effect of pH on substate fluctuations. Single channels were observed at a holding potential of −100 mV, in solutions adjusted symmetrically to the indicated pH values. Each trace is taken from a separate membrane.

indication of the molecularity of the proton activation. The slopes of the Hill plots are close to unity at all voltages studied, one of which is shown here; this result suggests that only one proton is involved in the proton-driven channel opening.

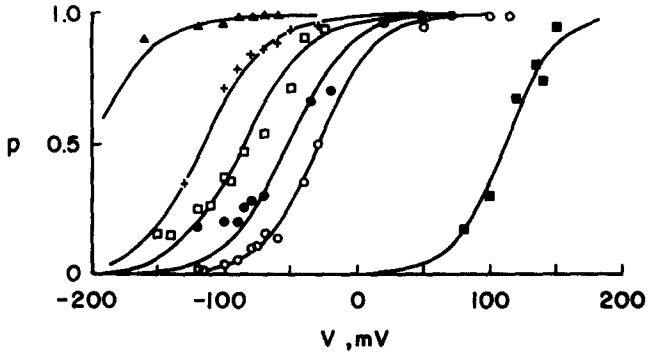

FIGURE 4. Protochannel activation probability: dependence on voltage and pH. Fundamental activation probability, p, of the individual protochannel was calculated from substate frequencies as in Figs. 2 and 3 via Eq. 3. Data at each pH value were fit to Eq. 8, with parameters given below. These are compiled data collected from 25 separate bilayers; data from 2–5 separate bilayers were used for each pH value, and each point represents the average of 2–4 data sets, each involving 100–1,000 fluctuations. (▲) pH 6.0, $V_o = -200$ mV, $z = 0.8$. (+) pH 7.0, $V_o = -116$ mV, $z = 1.0$. (□) pH 7.5, $V_o = -85$ mV, $z = 1.1$. (●) pH 8.0, $V_o = -52$ mV, $z = 1.1$. (○) pH 8.5, $V_o = -29$ mV, $z = -1.2$. (■) pH 10.4, $V_o = +62$ mV, $z = 1.3$.

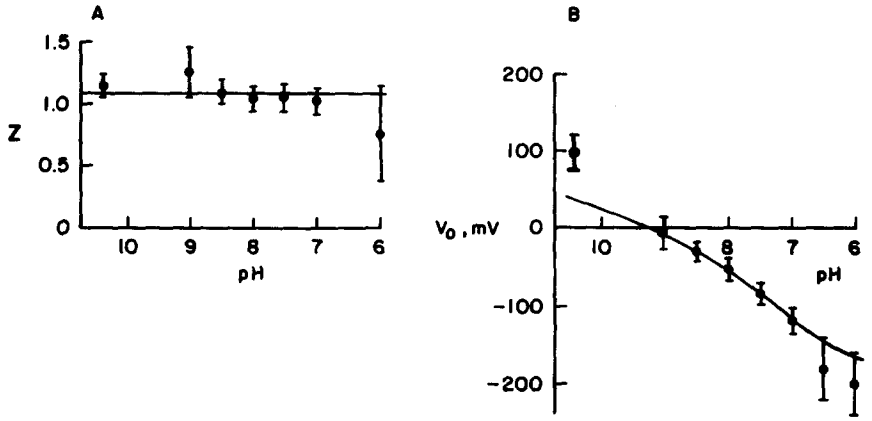

FIGURE 5. Protochannel opening parameters: dependence on pH. The effective gating charge z and half-saturation voltage V_o, determined as in Fig. 4, are displayed as a function of pH. The solid line was drawn empirically for the gating charge data (*A*). The curve through the V_o data was drawn according to Eq. 18. Parameters used for this fit were: $K_1(0) = 0.25$, $pK_o = 9.5$, $pK_c = 6.0$. Error bars were determined by rocking the linearized data of Fig. 4 by eye and noting the worst-case values.

The experiments above were carried out with symmetrical variation of pH, to eliminate the possibility of asymmetrical changes in surface potential as the PE amino group is titrated (pK = 9.5). However, all the effects of pH described here can be brought about by changing the pH only on the *cis* side of the bilayer. For example, no effect on rapid gating could be discerned when the *trans* pH was raised from 7.0 to 10.0 (data not shown); a similar variation in the *cis* pH lowers the equilibrium constant for opening 1,000-fold. Previous work (Miller and White, 1980) has documented the strong effects of *cis* pH on the macroscopic steady state conductance of bilayers containing many Cl^- channels.

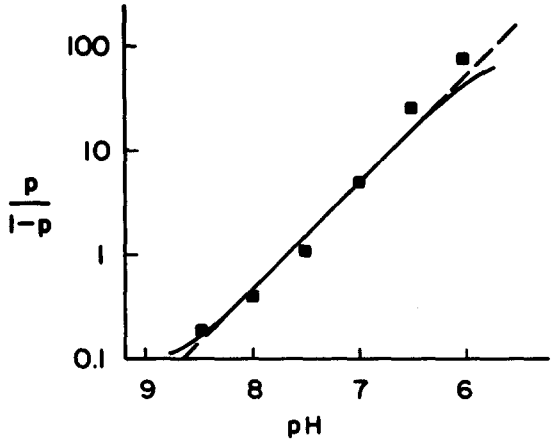

FIGURE 6. Hill plot for proton activation at −70 mV. Protochannel activation probability p was determined at −70 mV as in Fig. 3, at pH values indicated, to generate the Hill plot shown. The solid curve is drawn according to Eq. 11, with $K_1(-70\ \text{mV}) = 0.04$, $pK_o = 9.0$, $pK_c = 5.0$. The dashed line is drawn for reference with a slope of unity.

Effects of Voltage and pH on Gating Kinetics

To develop a picture of the activation of Cl^- channels by protons, it is necessary to supplement the above results on gating equilibrium with similar studies on gating kinetics. The probability distributions of all three substates were found to be single-exponential (Fig. 7). From the mean dwell times in the three substates, we can calculate the rates of opening and closing of the individual protochannel via Eq. 6 or Eq. 7, as in Table I. In Figs. 8 and 9, we see that both fundamental rate constants depend on voltage and pH. At all pH values, opening and closing rate constants vary exponentially with voltage. At all voltages, both the opening and closing rate constants vary with proton activity, but not in a simple way. As proton activity increases, the closing rate constant decreases to a limiting value below pH 6; this saturation is more clearly apparent in a reciprocal plot of the data (Fig. 9*C*). The existence of a limiting value for

μ at high pH is also suggested. The opening rate constant is an increasing function of proton activity; a limiting value at high pH is apparent, but if a low-pH asymptote exists, it is too rapid to be detected by our recording system. Below, we will see that this behavior of the rate constants allows us to choose a minimal model for the gating of the protochannel.

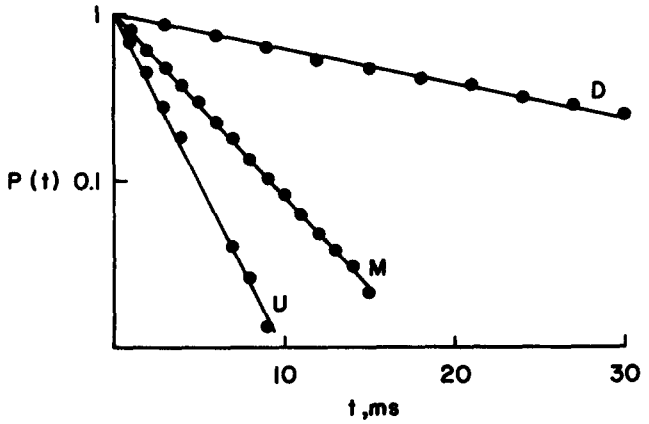

FIGURE 7. Time distributions of Cl^- channel substates. Single-channel dwell-time distributions in the indicated substates were determined at −85 mV and pH 7.5, as described in Materials and Methods. Time constants in this experiment were 19, 5, and 3 ms for the D, M, and U states, respectively; mean times and time constants agreed within 5% error. Probability, $P(t)$, is plotted as a cumulative distribution based on 1,659 total events.

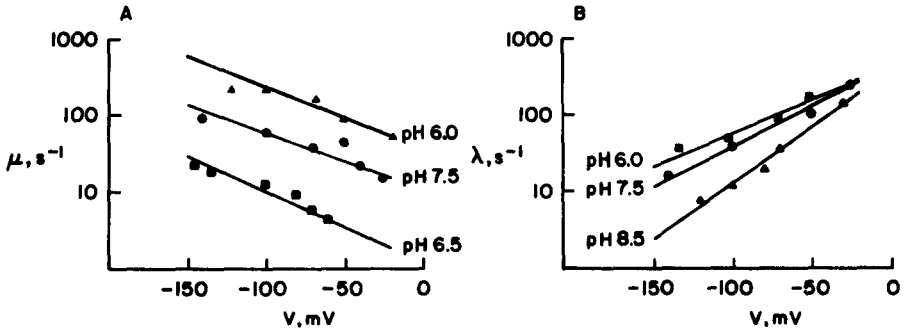

FIGURE 8. Voltage dependence of opening and closing rate constants. Rate constants for opening, λ, and closing, μ, were determined from substate fluctuation kinetics at the indicated pH values, according to Eqs. 6 and 7. Each point represents data taken from two to three separate bilayers.

DISCUSSION

In attempting to understand the gating of the *Torpedo* Cl^- channel, we have encountered two types of complications. The first is the existence of two gating processes in this channel. The slow process, on the time

scale of seconds, has been previously studied (White and Miller, 1979; Miller and White, 1980) and does not concern us here; only the fast process is presently under study. Although it is easy to distinguish the two gating processes by virtue of the different time scales in which they operate, an additional complication arises in trying to study the fast gating

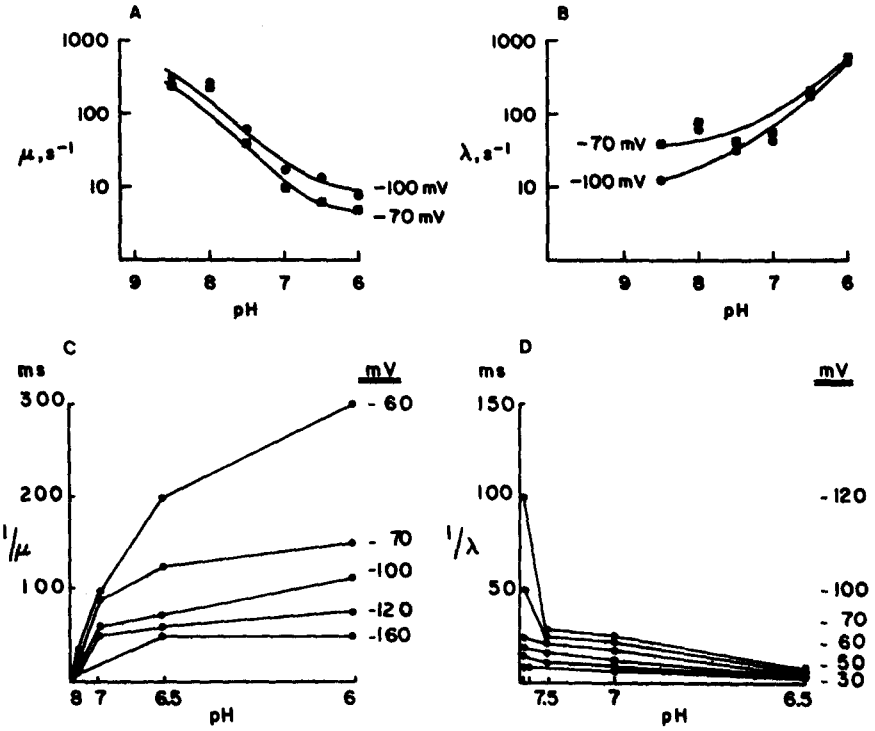

FIGURE 9. Opening and closing kinetics: dependence on pH. Rate constants for opening and closing were measured as in Fig. 8, at the indicated voltages as a function of pH. Solid curves are drawn according to Eq. 19, with the following parameters: $pK_o = 9.0$, $pK_c = 5.9$, $\mu_1 = \lambda_2 = 1{,}000\ s^{-1}$, for both voltages; $\mu_2(-70) = 4\ s^{-1}$, $\mu_2(-100) = 7\ s^{-1}$; $\lambda_1(-70) = 30\ s^{-1}$, $\lambda_1(-100) = 10\ s^{-1}$. (*A*) Closing rate; (*B*) opening rate; (*C*) more extensive data for closing rate, plotted on a reciprocal-linear scale, to illustrate the limiting value at low pH; (*D*) as in *C*, for opening rate.

behavior. It appears as though two separate "protochannels" independently open and close to generate the three observed "substates" of the channel complex. Strong support for this dimeric model is presented in Table I. Given the validity of this explanation, we can then reduce our questions about the rapid gating behavior to a simpler level: how does the individual protochannel open and close? How do voltage and proton activity control the individual protochannel gating process? The remainder of this discussion deals only with the properties of the protochannel.

We emphasize that we do not observe protochannels in isolation; they always appear in pairs in the Cl^- channel complex. But by assuming the dimeric model is correct, we can extract information about the protochannel from the observed rapid gating among the three active-channel substates.

Protochannel Gating Scheme

Previously, Miller (1982) suggested that the individual protochannel operates by a simple voltage-dependent mechanism, involving only two states, open and closed. The strong effect of pH on the protochannel gating behavior rules out this proposal; since protonation as well as voltage can drive the channel open, we must postulate the existence of at least one additional state of the protochannel in which a protonation reaction occurs. The fact that the Hill coefficient for the proton activation effect is close to unity (Fig. 6) suggests that only a single proton participates in this reaction. The most complete scheme with only a single protonation site therefore forms the basis of this discussion:

$$\begin{array}{ccc} & \overset{\lambda_1}{} & \\ \mathrm{C} & \rightleftharpoons & \mathrm{O} \\ K_c \downarrow & \overset{\mu_1}{} & \uparrow K_o \\ & \underset{\lambda_2}{} & \\ \mathrm{CH} & \rightleftharpoons & \mathrm{OH} \\ & \underset{\mu_2}{} & \end{array} \qquad (9)$$

Here, C and CH refer to unprotonated and protonated states of the closed channel, and O and OH refer similarly to the open channel. Both closed states are assumed to have zero conductance, and both open states are assumed to have identical conductance (10 pS under experimental conditions here). The protonation equilibria are described by the acid dissociation constants for the closed and open states, K_c and K_o, respectively. Opening and closing rates are described for both the unprotonated (λ_1 and μ_1) and protonated (λ_2 and μ_2) channels. The corresponding equilibrium constants for opening are given by:

$$K_1 = \lambda_1/\mu_1 \qquad K_2 = \lambda_2/\mu_2. \qquad (10)$$

At a given pH, the observed gating behavior will represent a mixture of the gating processes of the "pure" unprotonated and "pure" protonated states. The behavior of each of these pure states is approached at the corresponding extreme of pH.

Gating Equilibrium

The equilibrium results on proton activation show that in the unprotonated channel the equilibrium lies more towards the closed state than in the protonated channel. This, in turn, requires that in the closed state

the titratable group have a lower pK than in the open state. The general scheme above can be used to predict the variation of opening probability with proton activity [H]:

$$p/(1 - p) = K_1(1 + [H]/K_o)/(1 + [H]/K_c), \quad (11)$$

where K_1, K_o, and K_c may all be voltage dependent. Since the Hill plot (Fig. 6) is linear in the range pH 6.5–8.5, analysis of Eq. 11 requires that $K_c > 10^{-6}$ M and $K_o < 10^{-9}$ M.

We also note that considerations of detailed balance demand that:

$$K_1K_c = K_2K_o, \quad (12)$$

which places constraints not only on the values of the K's, but also on their voltage dependences. In particular, we assume that each equilibrium constant varies with voltage according to:

$$K_i(V) = K_i(0)e^{z_iFV/RT}, \quad (13)$$

where z_i is the "effective gating charge" of the appropriate step in scheme 9. Then, Eq. 12 leads to the relation:

$$z_1 + z_c = z_2 + z_o. \quad (14)$$

This relation among the gating charges must hold in general; an observed gating charge, z_{obs}, can be defined as:

$$z_{obs} = \frac{RT}{F}\left\{\frac{d \ln [p/(1 - p)]}{dV}\right\}_{p=0.5}, \quad (15)$$

in analogy with the definition of gating charge in a two-state model (Ehrenstein et al., 1970). Therefore, we expect that in general z_{obs} will vary with pH, since introducing Eqs. 11 and 13 into Eq. 15, we get

$$z_{obs} = z_1 - \frac{z_o}{1 + \frac{K_o(0)e^{z_oFV_o/RT}}{[H]}} + \frac{z_c}{1 + \frac{K_c(0)e^{z_cFV_o/RT}}{[H]}}, \quad (16)$$

where V_o is the voltage for $p = 0.5$, and is implicitly given by Eq. 11. If the acid dissociation constants do not vary with voltage, then z_{obs} will be pH independent:

$$z_{obs} = z_1 = z_2 \text{ (for } z_o = z_c = 0). \quad (17)$$

Figs. 4 and 5 show that proton activity exerts a profound effect upon the position of the probability-voltage curve upon the voltage axis, but has no discernable influence on the steepness of the activation curves. This, in turn, suggests that the "conformational" equilibria contain all of the voltage dependence, and that the protonation reactions contain none.

The general scheme also allows us to predict the shift in V_o with proton activity. By noting that $p = ½$ at $V = V_o$, and assuming that the protonation reactions are independent of voltage, Eq. 11 leads to:

$$V_o = \frac{-RT}{z_{obs}F} \ln\left\{\frac{K_1(0)(1 + [H]/K_o)}{(1 + [H]/K_c)}\right\}. \quad (18)$$

The observed pH variation of V_o (Fig. 5*B*) is in good agreement with Eq. 18, with $K_c = 10^{-6}$ M and $K_o = 10^{-9.5}$ M, if we ignore the single point at pH 10.4. These values are similar to those derived above from the Hill plot (Fig. 6). Furthermore, the fit to Eq. 18 implies that $K_1(0) < 1.5$ and $K_2(0) > 1{,}500$.

We have modeled scheme 9 in detail (not shown) to examine more closely whether the acid dissociation constants might be substantially voltage dependent. We find that, at most, 10% of the gating charge could be contained in the protonation equilibria, to be consistent with both the pH dependence of V_o and the pH independence of z_{obs}. We can therefore validly place all the voltage dependence of the channel gating in the opening/closing reactions and can consider the protonation steps independent of voltage.

Gating Kinetics

A crucial piece of information not provided by the equilibrium measurements is the degree of communication among the four states. An analysis of the pH dependence of the single-protochannel kinetics is required to eliminate a number of simpler transition schemes that would be consistent with the equilibrium results. We represent the general model of scheme 9, in which all relevant states communicate, with a square diagram:

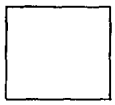

A kinetic scheme of this type predicts that the dwell-time distributions of both open and closed states should be double-exponential, in which both the amplitudes and rate constants of the exponential relaxations depend on pH (Colquhoun and Hawkes, 1981). We observe only single-exponential distributions for both open and closed times, a result requiring that the two protonation equilibria be rapid with respect to the two other reactions (Colquhoun and Hawkes, 1981). For example, this result rules out the two schemes

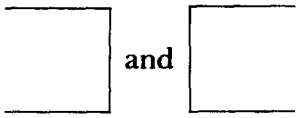

that demand that either the open or closed time show a double-exponential distribution, and that the amplitudes, but not the rate constants, of the exponentials vary with pH.

Other schemes are eliminated by the particular behavior of the opening and closing rate constants as a function of pH. Consider the sequential

scheme below in which only the unprotonated state of the channel can open and close:

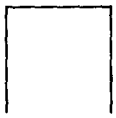

Here, single-exponential distributions are permitted if the protonation reactions are rapid compared with the opening and closing steps. But now both the opening and closing rates must vary inversely with proton activity. Experimentally, we do not observe this (Fig. 9). The opening rate actually increases strongly with proton activity, and the closing rate attains a minimum value at low pH, as is clearly shown in the reciprocal plot of Fig. 9*C*. Similarly, the complementary sequential scheme

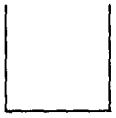

is eliminated by similar arguments. Simpler sequential models such as

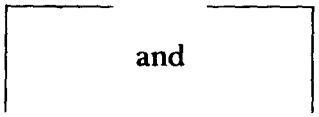

are also ruled out, since these demand that either the closing or opening rate constant be independent of pH.

The kinetic data, then, identify scheme 9 as the simplest model to explain the activation of the channel by protons. Assuming that both protonation equilibria are rapid (as implied by the observation of single-exponential time distributions), we can then write the variation of rate constant with H^+ activity:

$$\lambda([H]) = (\lambda_1 + \lambda_2[H]/K_c)/(1 + [H]/K_c) \quad (19a)$$

$$\mu([H]) = (\mu_1 + \mu_2[H]/K_o)/(1 + [H]/K_o) \quad (19b)$$

where the parameters are now independent of pH (but do, in general, vary with voltage). Both opening and closing rates are expected by Eq. 19 to reach limiting values at both high and low pH. These correspond to the opening and closing rates of the pure unprotonated or pure protonated channel, respectively. Over the voltage range −20 to −120 mV, limiting values for the opening rate at high pH, and the closing rate at low pH, are clearly indicated by our data (see Fig. 9 for an example). The values for these pure rate constants are shown in Fig. 10. Both vary exponentially with voltage, as expected for simple two-state behavior (Ehrenstein et al., 1974; Labarca et al., 1980). For the pure unprotonated channel, ~60% of the equilibrium gating charge, z_1, is contained in the opening rate λ; hence, 40% of the equilibrium voltage dependence lies in the closing rate μ_1. Similarly, for the pure protonated channel, 35% of

the equilibrium gating charge, z_1, resides in the closing rate μ_2, and 65% in the opening rate λ_2. Thus, the distribution of charge movement in opening and closing reactions appears similar for both protonated and unprotonated states of the channel.

Unfortunately, the opening rates at low pH and the closing rates at high pH increase beyond the time resolution of our system, and so only a hint of limiting values can be discerned. The measured opening rates and equilibrium constants, however, allow us to place limits on these

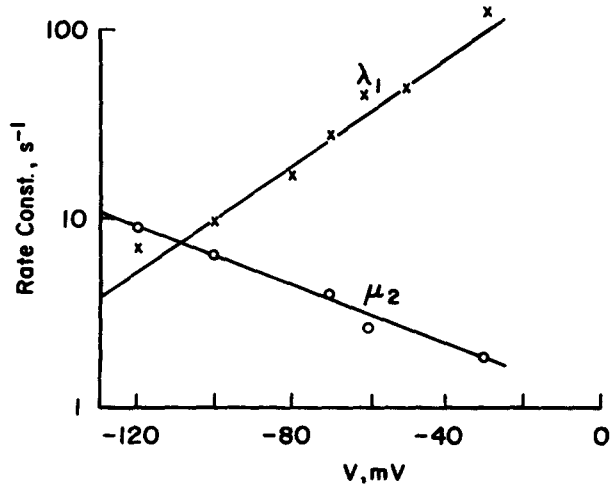

FIGURE 10. Voltage dependence of pure kinetic constants. Pure kinetic constants λ_1 and μ_2 were determined from data as in Fig. 9, by fitting Eq. 19, at the indicated voltages. Slopes of the lines drawn give the effective gating charge of the opening of the unpronated protochannel (0.65), and of the closing of the protonated channel (−0.35).

"invisible" rate constants. In Table II, best-fit values for the parameters are shown; the limiting rate constants λ_2 and μ_1 lie in the range 500–5,000 s^{-1}, just beyond the limit of resolution here.

We would like to know the voltage dependences of all the parameters in scheme 9. As shown above, the variations of λ_1 and μ_2 with voltage are easily determined. The voltage dependences of the "invisible" rate constants λ_2 and μ_1 are therefore determined from Eq. 14. We conclude that both opening rates λ_1 and λ_2 show nearly identical voltage dependences, though the absolute values differ by two orders of magnitude; similar conclusions hold for the closing rates, μ_1 and μ_2. It has not been possible to gather sufficiently accurate values for the acid dissociation constants to ascertain their voltage dependences. From our best determinations, we can say that K_o varies by <50% over the voltage range −120 to +50 mV. By Eq. 14, this must also be the case for K_c, since the observed gating charge is pH independent (Fig. 4). Thus, we again conclude that the acid

dissociation constants are independent of voltage, this time on the basis of kinetic evidence.

In Table II, we report values of the parameters of the four-state model most consistent with our data over the voltage range −120 to −20 mV from pH 6 to 10.4. These values provide an intuitively satisfying explanation for the effects of voltage and for activation of the channel by protons. Both the closed and open states of the channel can be protonated from the *cis* aqueous solution on a certain residue. Both the protonated

TABLE II

Equilibrium and Kinetic Parameters for Protochannel Gating

Equilibrium constants (−70 mV)		
From equilibrium	From kinetics	Effective charge
$pK_o = 9.0 \pm 0.5$	$pK_o = 8.0 \pm 0.5$	0
$pK_c = 6.0 \pm 0.5$	$pK_c = 5.5 \pm 0.5$	0
$K_1 = 0.1 \pm 0.02$	$K_1 = 0.05 \pm 0.02$	1.2±0.1
$K_2 = 150 \pm 50$	$K_2 = 250 \pm 50$	1.0±0.3

Rate constants (−70 mV)	Effective charge
$\lambda_1 = 32\ s^{-1}$	0.65
$\lambda_2 > 1{,}000\ s^{-1}$	0.60
$\mu_1 > 500\ s^{-1}$	−0.35
$\mu_2 = 4\ s^{-1}$	−0.4

Equilibrium constants, K_1, K_2, K_o, and K_c for four reactions of scheme 9 were determined from our most nearly complete data, taken at −70 mV, over the range pH 6–10.4. The best estimates shown were determined from fitting the equilibrium data from the Hill plot (Fig. 6) and from the pH-dependent shift of the half-saturation voltage (Fig. 5). Alternatively, equilibrium constants were calculated from the measured rate constants λ and μ at various pH values, using Eq. 5. Errors given in the reported values represent the range of parameters obtained by the various fits. Rate constants were similarly determined by the fit of the kinetic data at −70 mV to Eq. 19 (Fig. 9). Effective charge is given as a measure of the voltage dependence of the relevant parameter, as in Eq. 13.

and unprotonated states can undergo a conformational change between conducting and nonconducting states. Net charge movement occurs during this conformational change, so that voltage dependence is conferred upon these reactions; these charge movements are very similar for both protonated and unprotonated channels.

Biochemical Implications

Activation of the channel by protons is a direct consequence of the 1,000-fold difference in acid dissociation constant for the closed state vs. that of the open state. This difference requires that the closed state be greatly favored in the unprotonated channel [$K_1(-70\ mV) = 0.1$], whereas the open state is greatly favored in the protonated channel [$K_2(-70\ mV) = 150$]. It is important to realize that scheme 9 demands that the *same* titratable residue be involved in both open and closed states. In other

words, upon opening of the channel, a certain titratable group, exposed to the *cis* solution, changes its pK from 6 to 9. It is this change in pK that underlies the ability of protons to drive the channel into its open state.

The occurrence of a large change in acid dissociation constant coupled with a protein conformational change is not unusual in the biochemical literature. The classic example is the Bohr effect in hemoglobin, in which a histidine group increases its pK by 1 unit upon deoxygenation (Kilmartin and Rossi-Bernardi, 1973). More dramatic examples of altered pK values are found in superoxide dismutase (Stoesz et al., 1979), in which a histidine of pK 10.4 was observed (3.5 units higher than its "random coil" value); in chymotrypsin (Fersht, 1972), in which the terminal amino group pK is 10, a shift of 2 over units from its "unconstrained" value of 7.8; and in acetoacetate decarboxylase, in which a critical lysine pK is lowered from 9.2 to 6.0 (Kokesh and Westheimer, 1971). In each of these examples, the perturbed pK is the result of proximity of the titratable group to another charged residue.

Our results cannot identify the type of group involved in the pK change here, but biochemical precedent raises two reasonable possibilities. A lysine, of "normal" pK 9.2 in the open state, could be perturbed to pK 6 by proximity to a positively charged residue in the closed conformation. Alternatively, a "normal" histidine (pK 6.8) in the closed state could raise its pK to 9 by moving close to a negative group in the open state. Electrostatic calculations (Kirkwood and Westheimer, 1938) and experience with model compounds (Schwartzenbach, 1933) indicate that a lysine, for example, could decrease its pK by 3 units by approaching within 3.5 Å of a positively charged residue.

The possibility of a critical lysine of unusually low pK in the closed state tempts us to the following speculation. It is known that stilbene isothiocyanate derivatives inhibit this channel irreversibly from the *cis* side, probably by reacting with an unprotonated lysine residue (Miller and White, 1980). The rapid inhibition by these compounds suggests that the lysine involved is unusual, in that unconstrained primary amines do not react appreciably at neutral pH under the same conditions (M. White and C. Miller, unpublished data). We therefore propose that channel inhibition by these compounds is the result of covalent modification of a lysine of pK 6, the low-pK group of the closed channel (scheme 9). Such a reaction would lock the protochannel into the closed state, according to the four-state scheme. This hypothesis is entirely unsupported now, and its predictions are presently under investigation.

The physiological significance of this channel's control by pH and voltage is obscure. Conductances in the *Torpedo* electroplax noninnervated-face membrane have never been studied in detail, though it is known that during an electrical discharge, the voltage across this membrane remains constant (Bennett et al., 1961). Changes in pH in this system are uninvestigated. We think it likely that the behavior of the channel in this model membrane system is representative of its properties

in the native membrane. The channel's properties are quantitatively identical in three different model membrane systems: decane-containing planar bilayers (Miller, 1982), giant liposomes formed after detergent extraction of noninnervated-face vesicles (Tank et al., 1982), and, as we see here, solvent-free planar bilayers formed from lipid interface films. It is notable that macroscopic voltage-clamp studies on skeletal muscle (from which the electroplax evolved) present a rather complicated chloride conductance behavior: a chloride current inhibitable by stilbene isothiocyanate derivatives (Vaughan and Fong, 1978), which depends on both voltage and pH (Hutter and Warner, 1972; Loo et al., 1981). Further work is required to relate these chloride conductances, but qualitative similarities between the macroscopic currents and the *Torpedo* single-channel phenomena suggest more than a fortuitous connection.

The gating model introduced here is, in its essential points, similar to that developed to explain the activation by Ca^{++} of voltage-dependent K^+ channels from muscle plasma membranes (Methfessel and Boheim, 1982).[1] It is interesting that in the Ca^{++}-activated K^+ channel, all of the voltage dependence resides in the Ca^{++}-binding steps, and none in the opening and closing steps,[1] which is precisely the reverse of the activation of the Cl^- channel by protons. The overall similarities between the two systems identifies the *Torpedo* Cl^- channel as another example of a voltage-dependent, ion-gated ionic channel.

We are grateful to Dr. Ed Moczydlowski for cheerfully tolerating our frequent interruptions for advice on kinetic modeling of single-channel fluctuations, and to Dr. G. Menestrina for a critical reading of the manuscript.

This research was supported by National Institutes of Health Research Career Development Award (to C.M.) AM-00354 and by research grant R01-AM-19826. Dr. Hanke was in part supported by grant SFB114 of the Deutsche Forchungsgemeinschaft.

Received for publication 2 February 1983 and in revised form 29 March 1983.

REFERENCES

Bennett, M. V. L., M. Wurzel, and H. Grundfest. 1961. The electrophysiology of electric organs of marine electric fishes. I. Properties of electroplaques of *Torpedo nobeliana*. *J. Gen. Physiol.* 44:757–804.

Cohen, F. S., M. H. Akabas, and A. Finkelstein. 1982. Osmotic swelling of phospholipid vesicles causes them to fuse with a planar phospholipid bilayer membrane. *Science (Wash. DC)*. 217:458–460.

Cohen, F. S., J. Zimmerberg, and A. Finkelstein. 1980. Fusion of phospholipid vesicles with planar phospholipid bilayer membranes. II. Incorporation of a vesicular membrane marker into the planar membrane. *J. Gen. Physiol.* 75:251–270.

Colquhoun, D., and A. G. Hawkes. 1981. On the stochastic properties of ion channels. *Proc. R. Soc. B Biol. Sci.* 211:205–235.

[1] Moczydlowski, E., and R. Latorre. 1983. Gating kinetics of single Ca^{2+}-activated K^+ channels from rat muscle plasma membrane incorporated in planar bilayers: evidence for two voltage-dependent binding reactions. Manuscript submitted for publication.

Ehrenstein, G., R. Blumenthal, R. Latorre, and H. Lecar. 1974. Kinetics of the opening and closing of individual excitability-inducing material channels in a lipid bilayer. *J. Gen. Physiol.* 63:707–721.

Ehrenstein, G., H. Lecar, and R. Nossal. 1970. The nature of the negative resistance in bimolecular lipid membranes containing excitability-inducing material. *J. Gen. Physiol.* 55:119–133.

Fersht, A. R. 1972. Conformational equilibria in α- and Δ-chymotrypsin. The energetics and importance of the salt bridge. *J. Mol. Biol.* 64:497–509.

Hamill, O. P., A. Marty, E. Neher, B. Sakmann, and F. J. Sigworth. 1981. Improved patch-clamp techniques for high-resolution current recording from cells and cell-free membrane patches. *Pflügers Arch. Eur. J. Physiol.* 391:85–100.

Hutter, O. F., and A. E. Warner. 1972. The voltage dependence of chloride conductance of frog muscle. *J. Physiol. (Lond.).* 227:275–290.

Kilmartin, J. V., and L. Rossi-Bernardi. 1973. Interaction of hemoglobin with hydrogen ions, carbon dioxide, and organic phosphates. *Physiol. Rev.* 53:836–890.

Kirkwood, J., and F. H. Westheimer. 1938. The electrostatic influence of substituents on the dissociation constant of organic acids. I. *J. Chem. Phys.* 6:506–512.

Kokesh, F. C., and F. H. Westheimer. 1971. A reporter group at the active site of acetoacetate decarboxylase. II. Ionization constant of the amino group. *J. Am. Chem. Soc.* 93:7270–7274.

Labarca, P., R. Coronado, and C. Miller. 1980. Thermodynamic and kinetic studies of the gating behavior of a K-selective channel from the sarcoplasmic reticulum membrane. *J. Gen. Physiol.* 76:397–424.

Loo, D. F., J. G. McLarnon, and P. Vaughan. 1981. Some observations on the behavior of chloride current-voltage relations in *Xenopus* muscle membrane in acid solutions. *Can. J. Physiol. Pharmacol.* 59:7–13.

Methfessel, C., and G. Boheim. 1982. The gating of single calcium-dependent potassium channels is described by an activation/blockade mechanism. *Biophys. Struct. Mech.* 9:35–60.

Miller, C. 1982. Open-state substructure of single chloride channels from *Torpedo* electroplax. *Phil. Trans. R. Soc. B Biol. Sci.* 299:401–411.

Miller, C., and M. M. White. 1980. A voltage dependent chloride channel from *Torpedo* electroplax membrane. *Ann. NY Acad. Sci.* 341:534–551.

Montal, M., and P. Mueller. 1972. Formation of bimolecular membranes from lipid monolayers and a study of their electrical properties. *Proc. Natl. Acad. Sci. USA.* 69:3561–3566.

Schwartzenbach, G. 1933. Zur intramolekularer Atomabstande aus den Dissoziationskonstanten zweibasischer Sauren. *Helv. Chim. Acta.* 16:522–528.

Sobel, A., M. Weber, and J. P. Changeux. 1977. Large-scale purification of the acetylcholine receptor in its membrane-bound and detergent-extracted forms from *Torpedo mamorata* electric organ. *Eur. J. Biochem.* 80:215–224.

Stoesz, J. D., D. P. Malinowski, and A. G. Redfield. 1979. Nuclear magnetic resonance study of solvent exchange and nuclear overhauser effect on the histidine protons of bovine superoxide dismutase. *Biochemistry.* 18:4669–4675.

Taguchi, T., and M. Kasai. 1980. Identification of an anion channel protein from the electric organ of *Narke Japonica. Biochem. Biophys. Res. Commun.* 96:1088–1094.

Tank, D., and C. Miller. 1983. Patch-clamped liposomes: recording reconstituted ion

channels. *In* Gating of Single Ionic Channels. B. Sakmann and E. Neher, editors. Raven Press, New York. In press.

Tank, D., C. Miller, and W. W. Webb. 1982. Isolated-patch recording from liposomes containing functionally reconstituted chloride channels from *Torpedo* electroplax. *Proc. Natl. Acad. Sci. USA.* 79:7749–7753.

Vaughan, P., and C. N. Fong. 1978. Effects of SITS on chloride permeation in *Xenopus* skeletal muscle. *Can. J. Physiol. Pharmacol.* 56:1051–1054.

White, M. M. 1981. Characterization of a voltage-gated Cl^- channel from *Torpedo* electroplax. Ph.D. Dissertation, Brandeis University, Waltham, MA.

White, M. M., and C. Miller. 1979. Voltage-gated anion channel from electric organ of *Torpedo californica. J. Biol. Chem.* 254:10161–10166.

White, M. M., and C. Miller. 1981*a*. Probes of the conduction process of a voltage-gated chloride channel from *Torpedo* electroplax. *J. Gen. Physiol.* 78:1–19.

White, M. M., and C. Miller. 1981*b*. Chloride permeability of membrane vesicles isolated from *Torpedo* electroplax. *Biophys. J.* 35:455–462.